NATURAL CONVECTION IN SHALLOW AIR-FILLED ENCLOSURES - Part 2

الحمل الطبيعي في سياجات ضحلة مملؤة هواء - جزء (٢)

By
SHALABY, M.A.*, SHAHEEN, A.S., ** and EL-SEDEEK, A**
(*Mech. Engg. Dept**., Physical Science Dept.
Faculty of Engg., Mansoura University, Egypt)

الخلاصة : يتضمن هذا البحث دراسة عددية لمعدلات إنتقال الحرارة بالحمل الطبيعي داخل سياجات مستطيلة المقطع ضحله مملؤة هواء وذات نسب أعتبارية $0.1 \leq A \leq 1.0$ حيث يأخذ رقم ريلية القيمة من 10^3 إلى 10^6 ويأخذ رقم براندل بالهواء القيمة ٠,٧٣ . والسياجات محل الدراسة جدرانها الرأسية عند درجات حرارة ثابتة حيث أحد الجدران ساخن و الآخر بارد .
ولقد تمت الدراسة على أساس أن السريان رقائقي وفي أتجاهين ومستقر . ولقد ناقش البحث تأثير النسبة الإعتبارية للسياج على معدل الإنسياب الحرارى بالحمل الطبيعي . كما أجريت دراسة مقارنة بين النتائج التي حصلنا عليها والنتائج المتاحة عند الآخرين .

ABSTRACT - The heat transfer rates inside rectangular air closures of aspect ratios between 0.1 and 1.0 are studied numerically for a Rayleigh number ranges between 10^3 and 10^6 and Pr = 0.73. The shallow enclosures have isothermal hot and cold vertical walls. The flow is considerd to be two-dimensional, laminar and steady. The effect of the aspect ratio on the heat transfer and the natural convection flow is discussed. A comparison has been made with the available data in the literature.

INTRODUCTION

Rectangular enclosures containing air are commonly used to provide thermal insulation. Double pane windows and empty wall in frame construction houses are examples of rectangular enclosures. Shallow cavities are rectangular enclosures, but with small aspect ratios (enclosures that are wider than they are high). In the enclosures, one vertical wall is usually considered to be at a high temperature and the other vertical wall at a low temperature. The horizontal surfaces of the enclosure are normally treated as adiabatic surfaces. Heat is transferred between the two vertical walls by conduction and/or convection. A vast majority of research in enclosures has been aimed at high aspect ratio (A) enclosures perhaps because there are many applications of large aspect ratios enclosures. However, very few studies have been reported for enclosures of aspect ratios less than one. The available analytical and numerical studies were reported by Shiralkar and Tien [1], Boyack and Kearney [2], Cormack et.al. [3-5], and Bejan and Tien [6]. On the other hand, a considerable amount of works has been made for enclosures of aspect ratio equal to one. The numerical results have been reported by Wilkes and Churchill [7], de Vahl Davis [8], Shalaby, et.al. [9], MacGregor and Emery [10], Newell and Schimidt [11], and Briggs [12]. However, the numerical studies, except for Briggs [12] and Shalaby, et.al. [9] were limited by numerical stability to Rayleigh numbers (Ra) 2.2×10^5. Thus most of the available data for A = 1 are in the low Rayleigh number range.

This paper presents a study on the shallow cavity with different aspect ratios; A = 3/4, 1/2, 1/4 and 1/10. This study shows the effect of the aspect ratio on the Nusselt number, velocity profile stream lines and isotherms. The Rayleigh number values range between 10^3 and 10^6 and the Pr = 0.73.

FORMULATION OF THE PROBLEM

The problem considered is depicted schematically in Fig. (1) and referes to the two-dimensional flow in a shallow cavity. The cavity is assumed to be of infinite depth along the z-axis. The hot and cold vertical walls are considered to be isothermal and the other two adiabatic. The resulting flow is treated as steady and depending on the Rayleigh number (Ra). The compressibility of the fluid is negligible and there is no heat generation, so $\rho = c$ and $q_v = 0$. The temperature difference $(T_h - T_c)$ is small compared to the absolute temperature T_c of the cold boundary, so the viscosity, specific heat and thermal conductivity are constants and the density is also constant except for the effect of its variation in producing buoyancy forces.

Based on the above considerations, the set of partial differential equations governing laminar free convection flow in the cavity are formulated in dimensionless form, taking the cavity height as a characteristic length. The governing equations are presented as follows;

continuity

$$\frac{\partial U}{\partial X} + \frac{\partial V}{\partial Y} = 0 \qquad (1)$$

X - direction momentum

$$U \frac{\partial U}{\partial X} + V \frac{\partial U}{\partial Y} = - \frac{\partial P}{\partial X} + \frac{\partial^2 U}{\partial X^2} + \frac{\partial^2 U}{\partial Y^2} \qquad (2)$$

Y - direction momentum

$$U \frac{\partial V}{\partial X} + V \frac{\partial V}{\partial Y} = - \frac{\partial P}{\partial Y} + \frac{\partial^2 V}{\partial X^2} + \frac{\partial^2 V}{\partial Y^2} + Gr\ \theta \qquad (3)$$

$$U \frac{\partial \theta}{\partial X} + V \frac{\partial \theta}{\partial Y} = - \frac{1}{Pr} \left(\frac{\partial^2 \theta}{\partial X^2} + \frac{\partial^2 \theta}{\partial Y^2} \right) \qquad (4)$$

and the boundary conditions are:

Top wall : $Y = 1$ $\quad U = 0,\ V = 0,\ \frac{\partial \theta}{\partial Y} = 0$ (5)

Bottom wall: $Y = 0$ $\quad U = 0,\ V = 0,\ \frac{\partial \theta}{\partial Y} = 0$ (6)

Left side: $X = 0$ $\quad U = 0,\ V = 0,\ \theta = 1$ (7)

Right side: $X = A$ $\quad U = 0,\ V = 0,\ \theta = 0$ (8)

The dimensionless governing equations (1 - 4) in the primitive variable form are solved on rectangular meshes with 34 X 34 grids in the domain. Finite difference equations are derived by integration of the differential equations over a small rectangular control volume. The power-law difference scheme is used for the finite difference coefficient computations.

The finite difference equations are solved using line-by-line procedure. The used method is the alternating direction implicit (ADI) procedure with under-relaxation. Each one of the fields, U,V, P and θ is advanced after each iteration until the convergence criteria is achieved ($\xi \leq 5 \times 10^{-4}$), and an overall energy balance is satisfied. The details of the numerical derivation are mentioned in [13,14].

RESULTS AND DISCUSSION

As a test problem for the numerical method and the grid size, we considered the case of the square cavity as mentioned in [14].

The numerical solutions were carried out over Ra values range from 10^3 to 10^6 The other controllable variable in the numerical solutions was the aspect ratio which was varied from 0.1 to 1.0. The main results are presented in graphical and tabular form, and as Nu vs Ra correlations. The solution were computed for Pr = 0.73 (air). The present values of Nusselt number are correlated by the least square linear regression as follows:

$$Nu = a\, Ra^{b} \qquad (9)$$

where a and b are constants. This correlation fit the numerical results, obtained within 0.5 %.

Table (1) shows the obtained values of the constants a and b of the correlation (9) corresponding to the aspect ratio (A).

Table (1) Constants of Correlation (9)

A	a	b
1	0.142	0.302
3/4	0.1223	0.3112
1/2	0.1002	0.3243
1/4	0.0456	0.3715
1/10	0.0016	0.5975

The constants a and b were obtained for the square cavity (A =1) when Ra ranges from 10^3 to 10^7, but for the other aspect ratios when Ra ranges from 10^3 to 10^6. Fig. (2) presents the Nusselt number versus the Rayleigh number values at different aspect ratios. It is seen that, as the aspect ratio, for the enclosure, decreases the corresponding Nusselt number values decreases. One may also observe that, there is no significant difference between the Nu values obtained for the aspect ratio range from 0.5 to 1.0. However, there is a significant decrease in the Nu values as the

aspect ratio decreases to be equal to 1/4 and 1/10. The figure shows that, the plotted Nu values in general, increase with Ra. However, the heat transfer data show some asymptotical effect with the increase of Ra.

FLOW REGIMES

Fig. (3-left) illustrates the isotherms for Ra = 10^5 and at A = 3/4, 1/2 and 1/10. These lines are plotted in uniform increments equal to 0.1. In Fig. (3-a), at A = 3/4, the isothermal lines are vertical at the ends of the walls and are parallel to the vertical sides. These lines are concentrated at the starting ends of the boundary layer in which the local heat transfer coefficients are higher than the corresponding values at the departure corners of the boundary layer. On the other side, the isotherms have a negative slope at the center of the cavity. However, as the cavity becomes a little more shallow (A = 0.5) the isotherms at its core become more horizontal as seen in Fig. (3-b-left). The above observation, means that the boundary layer regime starts, i.e. $(\partial \theta / \partial X) = 0$, at the cavity center. It is also seen that the temperature in the vertical direction in the core region depends almost linearly on Y and the temperature gradient in vertical direction is positive. As the aspect ratio of the enclosure decreases to be 0.1, as seen in Fig. (3-c-left) the isotherms become almost vertical. This means that the boundary layer flow is vanished and the secondary flow exists in the cavity, and the main flow of heat takes place between the two vertical walls by conduction.

Fig. (3-right) also shows the contour maps of stream lines for A = 0.75, 0.5 and 0.1 at Ra = 10^5. The stream lines are plotted in uniform increments of $\Delta\psi$ which is different for each aspect ratio, for example $\Delta\psi$ equals to 1.5 for the case of A = 0.75 and 0.5 decreases to be equal to 0.1 for the cavity A = 0.1. On the other hand, the maximum stream lines strength inside the consisted vortices are 11.5, 8.5 and 0.5 for the enclosures of aspect ratios equal to 0.75, 0.5 and 0.1 respectively. One may observe that the fluid motion decreases sharply as the aspect ratio of the enclosure varied from 0.75 and 0.5 and 0.1. This means that the most of heat transferred between the two vertical walls takes place by conduction, i.e. the more shallow cavity is a good thermal insulation. One may also observe that, in the domain of the enclosure of aspect ratio euqal to 0.75 there is only one eddy existed, but it takes place near the hot side. As the aspect ratio becomes 0.5 the core of the cavity seems to have two eddies. This observation becomes clear when the aspect ratio decreases to be equal to 0.1 in which one may observe that there are two eddies existed so closed to the vertical sides and separated by a semi stagnant zone. These types of the secondary motion occur at small aspect ratio A = 0.1 and cause a tertiary motion located between the secondary motion described above. This tertiary motion appears more clear in the domain of the enclosure at Ra = 10^6 The secondary motion has the same rotation as the primary motion, while the tertiary motion rotates in the opposite direction [14]. It appears that this type of secondary motion has an important effect on the stratification in the core region. The stratification in the side wall region produces the secondary motion and causes a decrease of the buoyancy force, but as long as the buoyancy force exceeds the viscous forces, there is an acceleration of the upward moving fluid.

COMPARISON WITH AVAILABLE DATA

The results obtained in the present paper are plotted in Fig. (4), for A = 0.1, in comparison with the same obtained by Shiralkar and Tien [1]. The figure shows a quite good agreement between the present data and the same of [1].

Fig. (5) shows the Nusselt number value versus the aspect ratio. The figure has the present data (for the shallow cavity) as well as the data obtained in part-I for the long enclosure of the same authors [14], for Ra ranges between 10^3 and 10^6. It is seen that the Nu value increases with the increase of A to have the maximum value at A = 1. And then, the figure shows that as the aspect ratio increases more than unity the Nu value starts to decrease with the increase of A. One may also observe that the Nu value increases with Ra and the aspect ratio effect becomes less at the higher values of Ra.

NOMENCLATURE

A	aspect ratio, (H/L), (from 0.1 to 1),
a,b	correlation constants,
Cp	specific heat,
g	acceleration of gravity,
Gr	Grashof number ($g\beta \Delta T H^3 / \nu^2$),
H	cavity height,
h	heat transfer coefficient,
k	thermal conductivity of fluid.
L	cavity width,
l_0	scale for length,
Nu	average Nusselt number, (hH/k),
Ra	Rayleigh number (Gr. Pr),
P	dimensionless pressure, $p / (\rho u_0^2)$,
Pr	Prandtl number, $(\mu Cp / k)$,
T	temperature,
T_o	reference temperature.
ΔT	characteristic temperature difference,
U,V	component of dimensionless velocity in X and Y direction respectively, $\frac{u}{u_0}$, $\frac{v}{u_0}$,
u_o	scale for velocity.
X,Y	Dimensionless distances in x and y cartesian coordinates, x/l_o, y/l_o.

GREEK LETTERS

β	volumetric expansion coefficient,
θ	dimensionless temperature $(T-T_o/\Delta T)$,
ρ	fluid density,
μ	dynamic viscosity,
ν	kinematic viscosity,
ψ	stream function

SUBSCRIPTS

c	cold side,
h	hot side,

REFERENCES

1. Shiralkar, G.S. and Tien, C.L., "A Numerical Study of Laminar Natural Convection in Shallow Cavities", ASME. Jr. Heat Transfer, Vol. 103, pp. (226-231), (1981).

2. Boyack, B.E., and Kearney, D.W., "Heat Transfer by Laminar Natural Convection in Low Aspect Ratio Cavities", ASME paper 72-Ht-52, presented at the AIChE- ASME Heat Transfer Conference Denver, Co, Aug. (1972).

3. Cormack, D.E., Leal, L.G., and Imberger, J. "Natural Convection in a Shallow Cavity with Differentially Heated End Walls. Part 1. Asymptotic Theory." Jr. Fluid Mechanics, Vol. 65, pp. (209-229), (1974).

4. Cormack, D.E., Leal, L.G.; and Seinfeld, J.H., "Natural Convection in a Shallow Cavity with Diffrentially Heated End Walls. Part 2. Numerical Solutions," Jr. Fluid Mechanics, Vol. 65, pp. (231-246), (1974).

5. Cormack, D.E., Stone, G.P., and Leal, L.G., "The Effect of Upper Surface Conditions on Convection in a Shallow Cavity with Differentially Heated End Walls," Int. Jr. Heat and Mass Transfer, Vol. 18, pp. (635-648), (1975).

6. Bejan, A., and Tien, C.L., "Laminar Natural Convection Heat Transfer in a Horizontal Cavity with Different End Temperatures," ASME Jr Heat Transfer, Vol. 100, pp. (641-647), (1978).

7. Wilkes, J.O., and Churchill, S.W., "The Finite-Difference Computation of Natural Convection in a Rectangular Enclosure, "AIChE Jr. Vol. 12, No. 1, p. 161, (1966).

8. de Vahl Davis, G., "Laminar Natural Convection in an Enclosed Rectangular Cavity," Int. Jr. Heat and Mass Transfer, Vol. 11, 1975-1693, (1968).

9. Shalaby, M.A., Gaitonde, U.N. and Sukhatme, S.P., "Laminar Natural Convection in an Enclosed Square Cavity," Jr. Thermal Engineering, Vol. 3, pp. (72-82), (1983).

10. MacGregor, R.K., and Emery, A.F., "Free Convection Through Vertical Plane Layers-Moderate and High Prandtl Number Fluids", ASME Journal of Heat Transfer, Vol. 91, No. .3, pp (391-403), (1969).

11. Newell, M.E., and Schmidt, F.W., "Heat Transfer by Laminar Natural Convection within Rectangular Enclosures," ASME Jr. Heat Transfer, Vol. 92, No.1, pp. (159-168), (1970).

12. Briggs, D.G., "Numerical Solutions of High Rayleigh Number Two-Dimensional Free Convection in Enclosures with an Aspect Ratio of One," Proceedings of AICA Int. Symposium of Computer Methods for Partial Differential Equations, Lehigh University, Bethlehem, PA, June (1975).

13. Shaheen, A.S.A., "Numerical Solution of the Natural Convection Heat Transfer Problems," M.Sc, Thesis, Mansoura University, Egypt (1989).

14. Shalaby, M.A., Saddek, A. and Shaheen, A.S.A., "Natural Convection in Vertical Air Filled Enclosures-Part 1," to be published in MEJ.

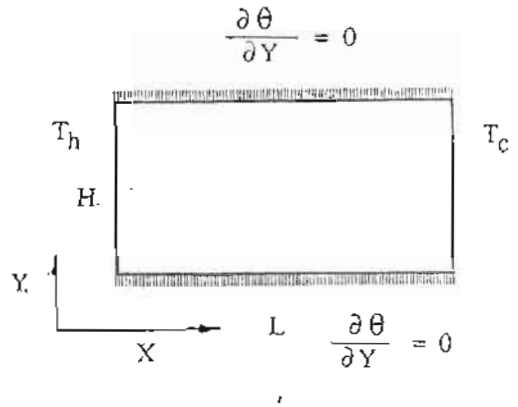

Fig. (1) Geometry of Shallow Cavity

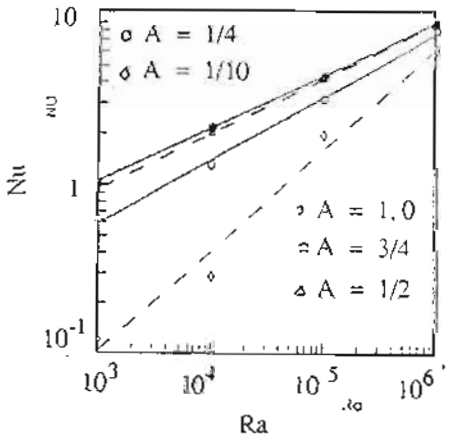

Fig. (2) Nusselt Number Versus Rayleigh Number at Different Aspect Ratios

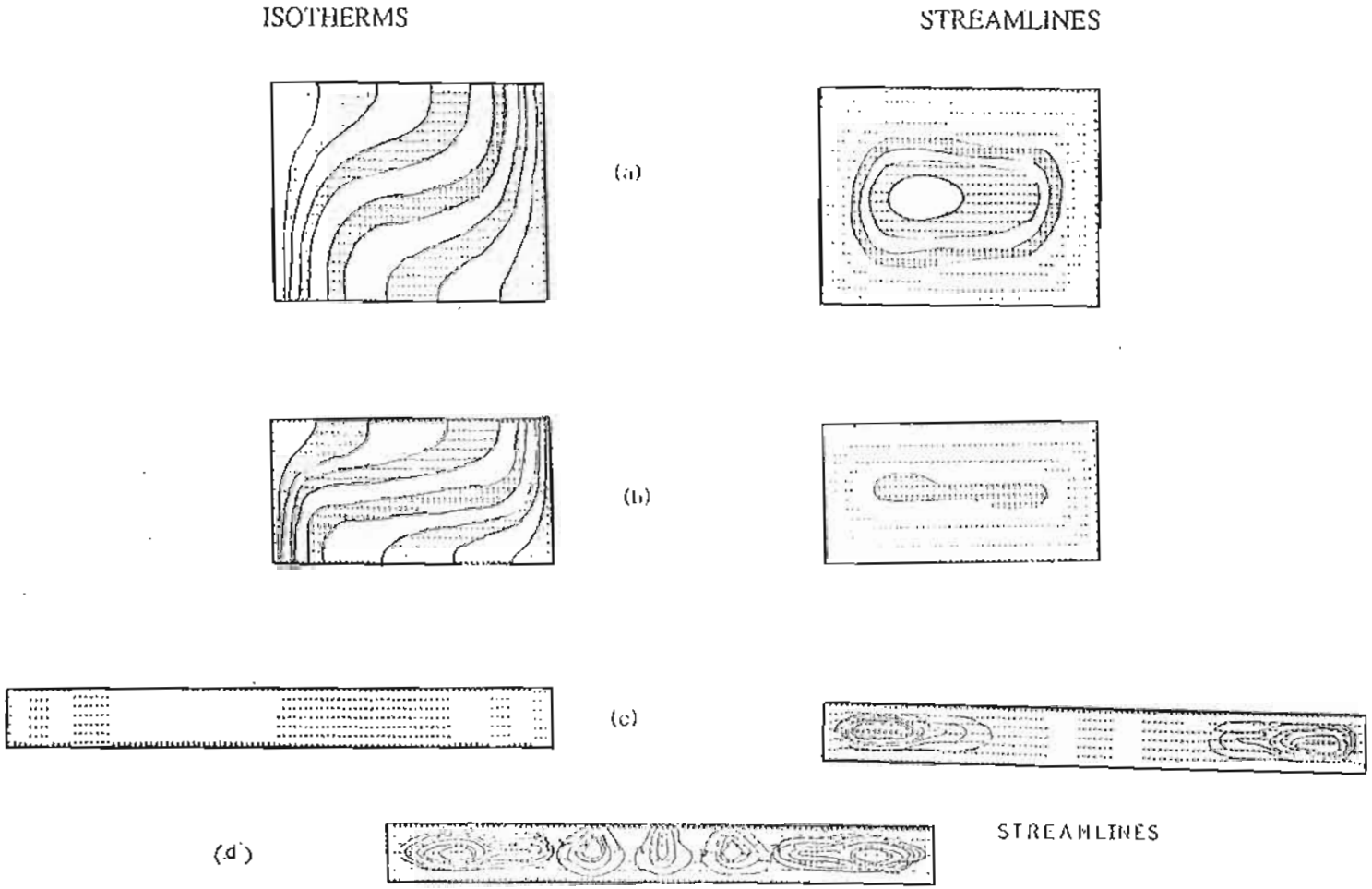

Fig. (3) Some Typical Examples of Isotherms (Left) and Streamlines (Right) at Ra = 10^5 for
(a) A = 0.75 (b) A = 0.5 and (c) A = 0.1,
(d) A = 0.1 at Ra = 10^6

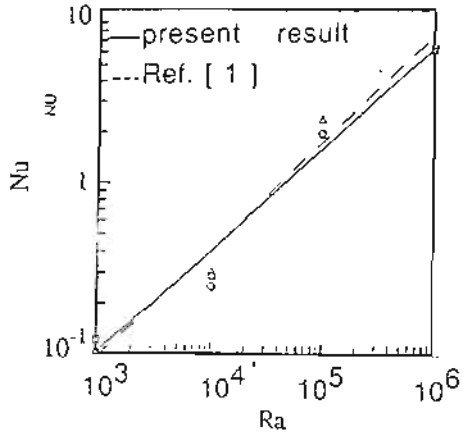

Fig (4) Nusselt Number Versus Rayleigh Number as a Comparison with Shiralkar [1] for A=0.1

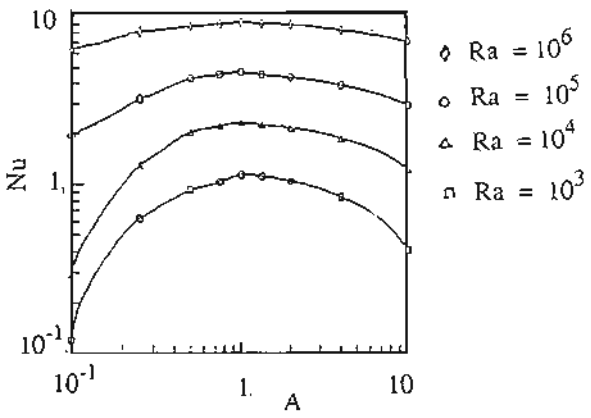

Fig. (5) Nusselt Number Versus Aspect Ratio